DOI 10.2478/ama-2023-0023

EFFECTIVE SHAPING OF A STEPPED SANDWICH BEAM WITH CLAMPED ENDS

Krzysztof MAGNUCKI*, Joanna KUSTOSZ*, Damian GOLIWĄS*

*Łukasiewicz Research Network – Poznan Institute of Technology, Rail Vehicles Center,
ul. Warszawska 181, 61-055 Poznań, Poland

krzysztof.magnucki@pit.lukasiewicz.gov.pl, joanna.kustosz@pit.lukasiewicz.gov.pl, damian.goliwas@pit.lukasiewicz.gov.pl

received 25 November 2022, revised 10 January 2023, accepted 10 January 2023

Abstract: The aim of this work is to propose a sandwich beam with stepped layer thickness in three parts along its length. The total depth, width of the cross-section and its mass are constant. The beam is under a uniformly distributed load. The system of two equilibrium equations was formulated for each part based on the literature. This system was analytically solved for the successive parts of the beam and the functions of the shear effect and deflection were determined in them. The effective stepped layer thicknesses was determined on the basis of the adopted criterion for minimizing the maximum deflection of the beam. The example calculations were made for two elected beams. The effective shapes of these beams are shown in the figures. Moreover, FEM numerical calculations of the deflections of these beams are performed.

Key words: analytical modelling, bending, shaping criterion, FEM calculation

1. INTRODUCTION

Sandwich constructions initiated in the 20th century are intensively developed in the 21st century. Vinson [1] presented a general introduction to the mechanics of sandwich structures with reference to the 174 articles. Icardi [2] developed a sublaminate model taking into account the zig-zag theory for the analysis of laminated and sandwich beams. The aim is to show the advantages of using higher-order approximations of displacements in sublaminates. Yang and Qiao [3] developed an analytical high-order impact model of a soft-core sandwich beam to analyse its response to foreign body impact. The results of analytical tests were compared with the results of FEM (Finite Element Method) numerical tests. Magnucka-Blandzi and Magnucki [4] presented the problem of effective shaping of a sandwich beam with a metal foam core with variable properties along its thickness. The optimal dimensionless parameters of the beam were determined on the basis of the adopted criterion. Kreja [5] described, based on a review of 246 articles, the state of the art in the field of analytical and numerical FEM methods used in the calculations of laminated composite and sandwich panels. Wang and Li [6] presented a theoretical analysis of bending of two types of sandwich beams with aluminium or steel facings and cores made of shape memory polymers. Nguyen et al. [7] studied sandwich panels with stepped facings and honeycomb cores. They have demonstrated in numerous examples that stepped linings can increase the strength and rigidity of sandwich structures. Phan et al. [8], taking into account the high-order theory of sandwich panels (HSAPT), developed a one-dimensional high-order theory for elastic orthotropic sandwich beams, taking into account the transverse compressibility of the core. Magnucki et al. [9] developed analytical and numerical FEM models of a five-layer sandwich beam and analysed its strength and stability. Sayyad and Ghugal [10] made a critical review of analytical and numerical studies described in selected 515 papers on bending, buckling and free vibration of homogeneous, laminated composite and sandwich beams, taking into account the applied theories. Birman and Kardomateas [11] presented, based on a review of 363 articles, contemporary trends in the development of sandwich structures in terms of theory and their practical application, with an emphasis on aviation, civil and marine engineering, electronics and biomedicine. In addition, sandwich structures are used in ships, which was described in detail by Kozak in 2018 [12]. Magnucki [13] presented analytical studies of bending of sandwich and I-beams with a symmetrical structure using two deformation models of flat cross-sections. Magnucki et al. [14] studied analytical and numerical FEM bending, buckling and free vibration of a sandwich beam with an asymmetric structure. The analytical model was developed taking into account the classic broken-line theory. Sayyad and Ghugal [15] presented a review of research, including 250 articles, on the modelling and analysis of functionally stepped sandwich beams and indicated directions for further research. Chinh et al. [16] analysed the bending of sandwich beams with a symmetrical structure with functionally stepped facings and a porous core subjected to a uniformly distributed load. Four types of supports for these beams, simply supported, clamped-clamped, clamped-hinged and clamped-free, were included. Magnucki et al. [17] developed three models of a simply supported sandwich beam and studied analytical and numerical FEM bending, buckling and free vibration. Kustosz et al. [18] analysed analytical and numerical FEM bending of a stepped sandwich beam with fixed ends under the action of a uniformly distributed load along its length. This work is a theoretical study presenting a generalized model of a sandwich beam, thanks to which it is possible to test the bending strength of beams with stepped structures.

The aim of this work is to propose the effective shaping of a

symmetrically stepped sandwich beam along its length. This work is a continuation of the studies presented in the paper [18].

2. ANALYTICAL STUDIES

2.1. Analytical model of the stepped sandwich beam

The subject of the studies is the sandwich beam stepped in three parts arranged symmetrically along its length. This beam with clamped ends of the length *L*, the total depth *h* and width *b* is subjected to the uniform load of intensity *q* (Fig. 1).

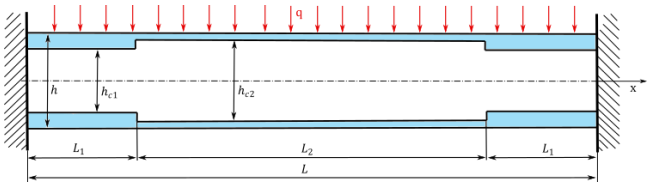

Fig. 1. Scheme of the stepped sandwich beam and the load

The volume of the core of the classical sandwich beam with constant layer thicknesses is given as follows

$$V_c^{(cl)} = bh_cL, \tag{1}$$

where h_c is the thickness of the core.

However, the volume of the core of the stepped sandwich beam (Fig. 1) is given in the following form:

$$V_c^{(st)} = b(2h_{c1}L_1 + h_{c2}L_2), \tag{2}$$

where h_{c1} is the thickness, L_1 is the length of the first part of the beam, h_{c2} is the thickness and L_2 is the length of the second-middle part of the beam.

Equating the volumes of the core of the classical beam (1) and the stepped beam (2), $V_c^{(cl)} = V_c^{(st)}$, after simple transformation, the following is obtained:

$$2\chi_{c1}\lambda_1 + \chi_{c2}\lambda_2 = \chi_c\lambda = \text{const}, \tag{3}$$

from which

$$\chi_{c2} = \frac{\chi_c\lambda - 2\chi_{c1}\lambda_1}{\lambda - 2\lambda_1}, \tag{4}$$

where $\chi_c = h_c/h, \chi_{c1} = h_{c1}/h, \chi_{c2} = h_{c2}/h$ is the relative thicknesses of the cores and $\lambda = L/h, \lambda_1 = L_1/h, \lambda_2 = L_2/h$ is the relative lengths of the beam and its parts, also $2\lambda_1 + \lambda_2 = \lambda$.

It is noted that the expression (3) also provides a constant volume of the faces, so it is a condition for constant mass of the stepped sandwich beam.

The system of two differential equations of equilibrium for individual parts of the stepped sandwich beam, based on the paper [18], is formulated in the following form:

$$C_{vvi}\frac{d^2\bar{v}^{(i)}}{d\xi^2} - C_{v\psi i}\frac{d\psi_f^{(i)}}{d\xi} = -6[(\xi - \xi^2)qL^2 - 2M_0]\frac{\lambda}{E_fbh^2}, \tag{5}$$

$$C_{v\psi i}\frac{d^3\bar{v}^{(i)}}{d\xi^3} - C_{\psi\psi i}\frac{d^2\psi_f^{(i)}}{d\xi^2} + C_{\psi i}\lambda^2\psi_f^{(i)}(\xi) = 0, \tag{6}$$

where $\xi = x/L$ is the dimensionless coordinate, $i = 1, 2$ is the number of the beam part, $\bar{v}^{(i)}(\xi) = v^{(i)}(\xi)/L$ is the relative deflection, $\psi_f^{(i)}(\xi)$ is the dimensionless longitudinal displacements in faces, $C_{vvi} = 1 - (1 - e_c)\chi_{ci}^3$, $C_{v\psi i} = 3 - (3 - 2e_c)\chi_{ci}^2$, $C_{\psi\psi i} = 4[3 - (3 - e_c)\chi_{ci}]$, $C_{\psi i} = \frac{24}{1+\nu_c}\frac{e_c}{\chi_{ci}}$, $e_c = E_c/E_f$ is the dimensionless coefficient, E_f, E_c is the Young modulus of faces and the core, ν_c is the Poisson ratio of the core and M_0 is the clamped-ends moment.

This system of two differential equations, Eqs (5) and (6), after simple transformation, is reduced to one differential equation in the following form:

$$\frac{d^2\psi_f^{(i)}}{d\xi^2} - (\alpha_i\lambda)^2\psi_f^{(i)}(\xi) = -6(1 - 2\xi)\frac{C_{v\psi i}}{C_{vvi}C_{\psi\psi i} - C_{v\psi i}^2}\lambda^3\frac{q}{E_fb}, \tag{7}$$

where $\alpha_i = \sqrt{\frac{C_{v\psi i}C_{\psi i}}{C_{vvi}C_{\psi\psi i} - C_{v\psi i}^2}}$ is the dimensionless coefficient.

The solution of this equation is given as the following function:

$$\psi_f^{(i)}(\xi) = k_{ci}[C_{1i}\sinh(\alpha_i\lambda\xi) + C_{2i}\cosh(\alpha_i\lambda\xi) + \\ +6(1 - 2\xi)]\lambda\frac{q}{E_fb}, \tag{8}$$

where $k_{ci} = \frac{C_{v\psi i}}{C_{vvi}C_{\psi i}}$ is the coefficient and C_{1i}, C_{2i} are integration constants.

Eq. (5), after the first integration, is given as follows:

$$C_{vvi}\frac{d\bar{v}^{(i)}}{d\xi} = C_{3i} + C_{v\psi i}\psi_f^{(i)}(\xi) - 6\left(\frac{1}{2}\xi^2 - \frac{1}{3}\xi^3 - \\ 2\xi\bar{M}_0\right)\frac{q\lambda^3}{E_fb}, \tag{9}$$

where C_{3i} is the integration constant and $\bar{M}_0 = M_0/qL^2$ is the dimensionless clamped-ends moment.

2.2. Analytical solution

The analytical solution is realized in the individual parts of the stepped beam.

The dimensionless longitudinal displacements in faces:

– the first part $(i = 1), 0 \le \xi \le \lambda_1/\lambda$

The function (8), with consideration of the boundary condition $\psi_f^{(1)}(0) = 0$, from which $C_{21} = -6$, is provided in the following form:

$$\psi_f^{(1)}(\xi) = k_{c1}[C_{11}\sinh(\alpha_1\lambda\xi) - 6\cosh(\alpha_1\lambda\xi) + \\ +6(1 - 2\xi)]\frac{q\lambda}{E_fb}. \tag{10}$$

This function for $\xi = \lambda_1/\lambda$ is as follows

$$\psi_f^{(1)}\left(\frac{\lambda_1}{\lambda}\right) = k_{c1}\left[C_{11}\sinh(\alpha_1\lambda_1) - 6\cosh(\alpha_1\lambda_1) + \\ 6\frac{\lambda_2}{\lambda}\right]\frac{q\lambda}{E_fb}, \tag{11}$$

– the second-middle part $(i = 2), \lambda_1/\lambda \le \xi \le 1/2$

The function (8), with consideration of the condition $\psi_f^{(2)}(1/2) = 0$ and simplification, is provided in the following form:

$$\psi_f^{(2)}(\xi) = 6k_{c2}(1 - 2\xi)\frac{q\lambda}{E_fb}. \tag{12}$$

DOI 10.2478/ama-2023-0023

Taking into account the continuity condition for the longitudinal displacements in faces $\psi_f^{(1)}(\lambda_1/\lambda) = \psi_f^{(2)}(\lambda_1/\lambda)$, the integration constant is obtained as follows:

$$C_{11} = \frac{6}{\sinh(\alpha_1\lambda_1)}\left[\cosh(\alpha_1\lambda_1) + \frac{k_{c2}-k_{c1}}{k_{c1}}\frac{\lambda_2}{\lambda}\right]. \tag{13}$$

Consequently, the function (10) is provided in the following form:

$$\psi_f^{(1)}(\xi) = 6k_{c1}\left\{-\frac{\sinh[\alpha_1(\lambda_1-\lambda\xi)]}{\sinh(\alpha_1\lambda_1)} + \frac{\sinh(\alpha_1\lambda\xi)}{\sinh(\alpha_1\lambda_1)}\frac{k_{c2}-k_{c1}}{k_{c1}}\frac{\lambda_2}{\lambda} + \right. \\ \left. +1-2\xi\right\}\frac{q\lambda}{E_f b}. \tag{14}$$

Therefore, the function for $\xi = \lambda_1/\lambda$ is given as follows:

$$\psi_f^{(1)}\left(\frac{\lambda_1}{\lambda}\right) = 6k_{c2}\lambda_2\frac{q}{E_f b} \tag{15}$$

The relative deflection:

– the first part $(i = 1)$, $0 \le \xi \le \lambda_1/\lambda$

Eq. (9), with consideration of the boundary condition $d\bar{v}^{(1)}/d\xi\,|_0 = 0$, from which $C_{31} = 0$, is provided in the following form:

$$C_{vv1}\frac{d\bar{v}^{(1)}}{d\xi} = C_{v\psi1}\psi_f^{(1)}(\xi) - 6\left(\frac{1}{2}\xi^2 - \frac{1}{3}\xi^3 - 2\xi\bar{M}_0\right)\frac{q\lambda^3}{E_f b}. \tag{16}$$

Therefore, the derivative of the relative deflection curve for $\xi = \lambda_1/\lambda$ is given as follows

$$\frac{d\bar{v}^{(1)}}{d\xi}|_{\frac{\lambda_1}{\lambda}} = \\ \left\{6C_{v\psi1}k_{c2}\frac{\lambda_2}{\lambda} - \left[\left(2+\frac{\lambda_2}{\lambda}\right)\frac{\lambda_1}{\lambda} - 12\bar{M}_0\right]\lambda_1\lambda\right\}\frac{q\lambda}{C_{vv1}E_f b}. \tag{17}$$

Eq. (16) after integration is given as follows:

$$C_{vv1}\bar{v}^{(1)}(\xi) = C_{41} + 6k_{c1}C_{v\psi1}\Phi_\psi^{(1)}(\xi)\frac{q\lambda}{E_f b} - \\ -6\left(\frac{\xi^3}{6} - \frac{\xi^4}{12} - \xi^2\bar{M}_0\right)\frac{q\lambda^3}{E_f b}, \tag{18}$$

where

$$\Phi_\psi^{(1)}(\xi) = \frac{\cosh[\alpha_1(\lambda_1-\lambda\xi)]}{\alpha_1\lambda_1\sinh(\alpha_1\lambda_1)} + \frac{\cosh(\alpha_1\lambda\xi)}{\alpha_1\lambda_1\sinh(\alpha_1\lambda_1)}\frac{k_{c2}-k_{c1}}{k_{c1}}\frac{\lambda_2}{\lambda} + \xi - \\ \xi^2. \tag{19}$$

Based on the boundary condition $\bar{v}^{(1)}(0) = 0$, the integration constant is given as follows:

$$C_{41} = -\frac{6k_{c1}}{\sinh(\alpha_1\lambda_1)}\frac{C_{v\psi1}}{\alpha_1\lambda}\left[\cosh(\alpha_1\lambda_1) + \frac{k_{c2}-k_{c1}}{k_{c1}}\frac{\lambda_2}{\lambda}\right]\frac{q\lambda}{E_f b}. \tag{20}$$

Therefore, the relative deflection of this part for $\xi = \lambda_1/\lambda$ is given as follows:

$$\bar{v}^{(1)}\left(\frac{\lambda_1}{\lambda}\right) = \left\{6k_{c1}C_{v\psi1}\left[\frac{k_0}{\alpha_1\lambda}\left(\frac{k_{c2}-k_{c1}}{k_{c1}}\frac{\lambda_2}{\lambda}-1\right) + \left(1-\frac{\lambda_1}{\lambda}\right)\frac{\lambda_1}{\lambda}\right] - \right. \\ \left. -\left[\frac{1}{2}\left(2-\frac{\lambda_1}{\lambda}\right)\frac{\lambda_1}{\lambda} - 6\bar{M}_0\right]\lambda_1^2\right\}\frac{q\lambda}{C_{vv1}E_f b}, \tag{21}$$

where $k_0 = \frac{\cosh(\alpha_1\lambda_1)-1}{\sinh(\alpha_1\lambda_1)}$ is the dimensionless coefficient.

– the second-middle part $(i = 2)$, $\lambda_1/\lambda \le \xi \le 1/2$

Taking into account Eq. (9) with consideration of the function (12), based on the condition $d\bar{v}^{(2)}/d\xi\,|_{1/2} = 0$, the integration constant is obtained as follows:

$$C_{32} = \frac{1}{2}(1 - 12\bar{M}_0)\frac{q\lambda^3}{E_f b}. \tag{22}$$

Therefore, Eq. (9) is provided in the following form:

$$C_{vv2}\frac{d\bar{v}^{(2)}}{d\xi} = \left\{6C_{v\psi2}k_{c2}(1-2\xi) + \left[\frac{1}{2} - 3\xi^2 + 2\xi^3 - \right.\right. \\ \left.\left. -6(1-2\xi)\bar{M}_0\right]\lambda^2\right\}\frac{q\lambda}{E_f b}. \tag{23}$$

Thus, the derivative of the relative deflection curve for $\xi = \lambda_1/\lambda$ is given as follows:

$$\frac{d\bar{v}^{(2)}}{d\xi}|_{\frac{\lambda_1}{\lambda}} = \left\{6C_{v\psi2}k_{c2}\frac{\lambda_2}{\lambda} + \left[\frac{1}{2} - \left(3-2\frac{\lambda_1}{\lambda}\right)\left(\frac{\lambda_1}{\lambda}\right)^2 - \right.\right. \\ \left.\left. -6\frac{\lambda_2}{\lambda}\bar{M}_0\right]\lambda^2\right\}\frac{q\lambda}{C_{vv2}E_f b}. \tag{24}$$

Based on the continuity condition for the derivative of the relative deflection curve $d\bar{v}^{(1)}/d\xi\,|_{\lambda_1/\lambda} = d\bar{v}^{(2)}/d\xi\,|_{\lambda_1/\lambda}$, the dimensionless clamped-ends moment is obtained as follows:

$$\bar{M}_0 = \frac{\mathrm{N}_{M0}}{12[2(C_{vv1}-C_{vv2})\lambda_1 - C_{vv1}\lambda]\lambda}, \tag{25}$$

where the numerator of this expression is given as follows:

$$\mathrm{N}_{M0} = 12\left(C_{vv2}C_{v\psi1} - C_{vv1}C_{v\psi2}\right)\frac{\lambda_2}{\lambda}k_{c2} - C_{vv1}\lambda^2 + \\ +2(C_{vv1} - C_{vv2})\left(2+\frac{\lambda_2}{\lambda}\right)\lambda_1^2. \tag{26}$$

Eq. (23) after integration is given as follows:

$$C_{vv2}\bar{v}^{(2)}(\xi) = C_{42} + \left\{6C_{v\psi2}k_{c2}(\xi-\xi^2) + \left[\frac{1}{2}\xi - \xi^3 + \right.\right. \\ \left.\left. +\frac{1}{2}\xi^4 - 6(\xi-\xi^2)\bar{M}_0\right]\lambda^2\right\}\frac{q\lambda}{E_f b}. \tag{27}$$

Based on the continuity condition for the relative deflection curve $\bar{v}^{(1)}(\lambda_1/\lambda) = \bar{v}^{(2)}(\lambda_1/\lambda)$, the integration constant is obtained as follows:

$$C_{42} = [6(\bar{C}_{421} - \bar{C}_{422}) - (\bar{C}_{423} + \bar{C}_{424})\lambda^2]\frac{q\lambda}{E_f b}, \tag{28}$$

where

$$\bar{C}_{421} = C_{v\psi1}\frac{C_{vv2}}{C_{vv1}}k_{c1}\left\{\frac{k_0}{\alpha_1\lambda}\left(\frac{k_{c2}-k_{c1}}{k_{c1}}\frac{\lambda_2}{\lambda}-1\right) + \left(1-\frac{\lambda_1}{\lambda}\right)\frac{\lambda_1}{\lambda}\right\},$$

$$\bar{C}_{422} = C_{v\psi2}k_{c2}\left(1-\frac{\lambda_1}{\lambda}\right)\frac{\lambda_1}{\lambda},$$

$$\bar{C}_{423} = \frac{C_{vv2}}{C_{vv1}}\left[\frac{1}{2}\left(2-\frac{\lambda_1}{\lambda}\right)\frac{\lambda_1}{\lambda} - 6\bar{M}_0\right]\left(\frac{\lambda_1}{\lambda}\right)^2,$$

$$\bar{C}_{424} = \left\{\frac{1}{2}\left[1+\left(1-\frac{\lambda_1}{\lambda}\right)\frac{\lambda_1}{\lambda}\right] - 6\bar{M}_0\right\}\left(1-\frac{\lambda_1}{\lambda}\right)\frac{\lambda_1}{\lambda}.$$

Taking into account Eq. (27), the maximum relative deflection of the stepped sandwich beam is given as follows:

$$\bar{v}_{\max} = \bar{v}^{(2)}\left(\frac{1}{2}\right) = \tilde{v}_{\max}\frac{q}{E_f b}, \tag{29}$$

where

$$\tilde{v}_{\max} = \left(\tilde{v}_\psi + \tilde{v}_v\lambda^2\right)\lambda, \tag{30}$$

and

$$\tilde{v}_\psi = 6\left\{\frac{C_{v\psi1}}{C_{vv1}}\frac{k_0}{\alpha_1\lambda}\left[(k_{c2}-k_{c1})\frac{\lambda_2}{\lambda} - k_{c1}\right] + \frac{1}{4}\frac{C_{v\psi2}}{C_{vv2}}k_{c2} + \right. \\ \left. +\left(\frac{C_{v\psi1}}{C_{vv1}}k_{c1} - \frac{C_{v\psi2}}{C_{vv2}}k_{c2}\right)\left(1-\frac{\lambda_1}{\lambda}\right)\frac{\lambda_1}{\lambda}\right\}, \tag{31}$$

DOI 10.2478/ama-2023-0023

$$\tilde{v}_v = \left(\frac{5}{32} - \frac{3}{2}\bar{M}_0 - \bar{C}_{423} - \bar{C}_{424}\right)\frac{1}{C_{vv2}}. \quad (32)$$

Thus, the criterion of effective shaping of the stepped sandwich beam was assumed as the minimization of the maximum dimensionless deflection of this beam, with considering two expressions (4) and $\lambda_2 = \lambda - 2\lambda_1$, and is obtained in the following form:

$$\min_{\lambda_1,\chi_{c1}}[\tilde{v}_{\max}(\lambda_1,\chi_{c1})]. \quad (33)$$

The detailed calculations are carried out for the exemplary stepped sandwich beams.

3. DETAILED CALCULATIONS

3.1. Beam B-1

The data of the classical sandwich beam B-1 are specified in Tab. 1. However, the results of the calculations, the effective dimensionless sizes and maximal deflection, are specified in Tab. 2.

Tab. 1. The classical sandwich beam – B-1

λ	e_c	ν_c	χ_c	$\tilde{v}_{\max}$
20	1/20	0.3	17/20	728.66

Tab. 2. The effective dimensionless sizes and maximal deflection – B-1

$\lambda_{1,ef}$	$\lambda_{2,ef}$	$\chi_{c1,ef}$	$\chi_{c2,ef}$	$\tilde{v}_{\max}$
2.4	15.2	14.66/20	17.74/20	676.02

Moreover, the graph of the dimensionless longitudinal displacements – shear effect functions (12) and (14) – is shown in Fig. 2, and the scheme of the effective shape of the stepped sandwich beam is shown in Fig. 3.

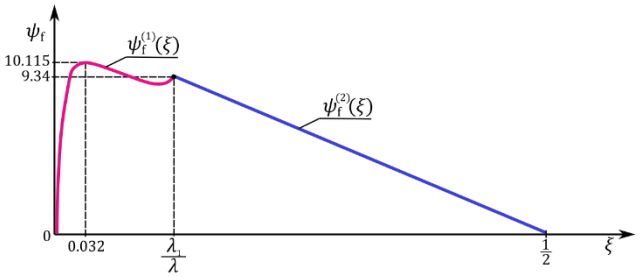

Fig. 2. The graph of the dimensionless longitudinal displacements – shear effect functions

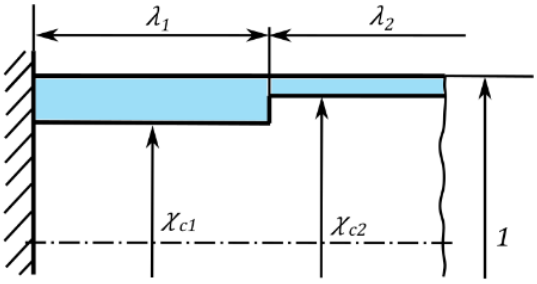

Fig. 3. The scheme of the effective shape of the stepped sandwich beam

3.2. Beam B-2

The data of the classical sandwich beam B-2 are specified in Tab. 3. Moreover, the results of the calculations, the effective dimensionless sizes and maximal deflection, are specified in Tab. 4, and the graph of the dimensionless longitudinal displacements – shear effect functions (12) and (14) – is shown in Fig. 4. The scheme of the effective shape of this stepped sandwich beam is similar to Fig. 3.

Tab. 3. The classical sandwich beam – B-2

λ	e_c	ν_c	χ_c	$\tilde{v}_{\max}$
20	1/20	0.3	16/20	613.14

Tab. 4. The effective dimensionless sizes and maximal deflection – B-2

$\lambda_{1,ef}$	$\lambda_{2,ef}$	$\chi_{c1,ef}$	$\chi_{c2,ef}$	$\tilde{v}_{\max}$
2.5	15.0	13.22/20	16.93/20	576.16

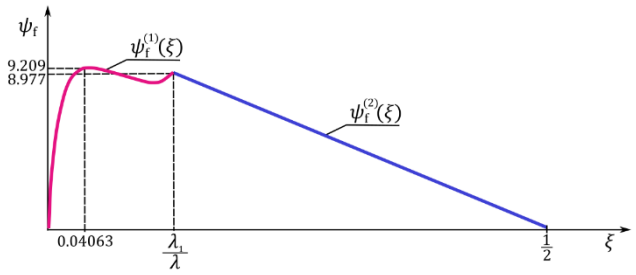

Fig. 4. The graph of the dimensionless longitudinal displacements – shear effect functions

4. NUMERICAL FEM STUDIES

4.1. Beam B-1

The numerical model of the example effective stepped sandwich beam B-1 was developed in the ABAQUS 6.12 system using 84,000 hexahedral linear finite elements (C3D8R type). The model of the beam is solid and represents only half of the beam due to the symmetry. The longitudinal x-axis is collinear with the beam neutral axis, the y-axis is directed and the z-axis is parallel to the cross-section of the beam. The beam is under a continuous load and its ends are clamped (Fig. 5).

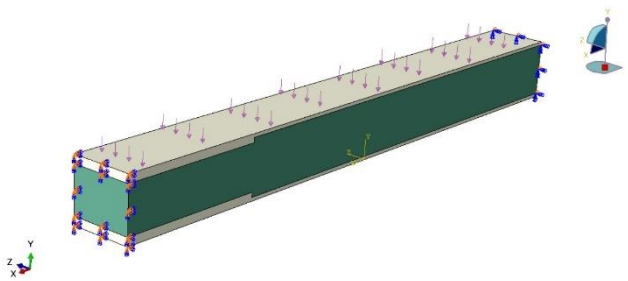

Fig. 5. The scheme of the numerical FEM model of the effective stepped sandwich beam B-1

DOI 10.2478/ama-2023-0023

The value of the maximum deflection determined numerically is as follows: $\tilde{v}_{\max} = 678.96$. The difference between analytical (An) and numerical (FEM) results is 0.43% in these exemplary stepped sandwich beam.

4.2. Beam B-2

The numerical model of the B-2 beam is analogous to the model of the B-1 beam. The value of the maximum deflection determined numerically is given as follows: $\tilde{v}_{\max} = 581.58$. The difference between analytical (An) and numerical (FEM) results is 0.94% in these exemplary stepped sandwich beams.

5. CONCLUSIONS

The detailed calculations for the exemplary stepped sandwich beams provide the following conclusions:

- The stiffness of the sandwich structures can be increased by introducing stepped facings, which is expressed in smaller maximum deflections compared to the maximum deflection of the classical sandwich beam, and so for the beam B-1 by 7.2% and for the beam B-2 by 6.0%.
- The developed analytical and numerical FEM models of this beam are equivalent, the differences between the values of the maximum deflections of the exemplary beams calculated based on these two models are less than 1%, and so for the beam B-1 is 0.43% and for the beam B-2 is 0.94%.
- The facings thicknesses of the effective sandwich beams in the first part, at clamped beam ends, are greater than the facings thicknesses in the middle part of these beams (Figs. 3 and 5).
- In future works related to this paper, the problem of effective shaping of sandwich beams with a stepped structure, taking into account the local buckling (face wrinkling), could be considered.

REFERENCES

1. Vinson JR. Sandwich structures. Applied Mechanics Reviews. 2001;54(3):201–214.
2. Icardi U. Applications of Zig-Zag theories to sandwich beams. Mechanics of Advanced Materials and Structures. 2003;10(1):77–97.
3. Yang M, Qiao P. Higher-order impact modeling of sandwich structures with flexible core. International Journal of Solids and Structures. 2005;42(20):5460–90.
4. Magnucka-Blandzi E, Magnucki K. Effective design of a sandwich beam with a metal foam core. Thin-Walled Structures. 2007;45(4):432-8.
5. Kreja I. A literature review on computational models for laminated composite and sandwich panels. Central European Journal of Engineering. 2011;1(1):59-80.
6. Wang ZD, Li ZF. Theoretical analysis of the deformation of SMP sandwich beam in flexure. Archive of Applied Mechanics. 2011;81(11):1667–78.
7. Nguyen CH, Chandrashekhara K, Birman V. Enhanced static response of sandwich panel with honeycomb cores through the use of stepped facings. Journal of Sandwich Structures and Materials. 2011;13(2):237-60.
8. Phan CN, Frostig Y, Kardomateas GA. Analysis of sandwich beams with a compliant core and with in-plane rigidity–extended high-order sandwich panel theory versus elasticity. ASME: Journal of Applied Mechanics. 2012;79:041001–1-11.
9. Magnucki K, Jasion P, Szyc W, Smyczynski M. Strength and buckling of a sandwich beam with thin binding layers between faces and a metal foam core. Steel and Composite Structures. 2014;16(3):325-37.
10. Sayyad AS, Ghugal YM. Bending, buckling and free vibration of laminated composite and sandwich beams: a critical review of literature. Composite Structures. 2017;171:486–504.
11. Birman V, Kardomateas GA. Review of current trends in research and applications of sandwich structures. Composites Part B. 2018;142:221-40.
12. Kozak J. Steel sandwich panels in ship structures. Gdańsk Tech Publishing House, 2018, Gdańsk. ISBN 978-83-7348-742-0 (in polish).
13. Magnucki K. Bending of symmetrically sandwich beams and I-beams – Analytical study. International Journal of Mechanical Sciences. 2019;150:411-9.
14. Magnucki K, Magnucka-Blandzi E, Lewiński J, Milecki S. Analytical and numerical studies of an unsymmetrical sandwich beam - bending, buckling and free vibration. Engineering Transactions. 2019;67(4):491-512.
15. Sayyad AS, Ghugal YM. Modeling and analysis of functionally graded sandwich beams: A review. Mechanics of Advanced Materials and Structures. 2019;26(21):1776-95.
16. Chinh TH, Tu TM, Duc DM, Hung TQ. Static flexural analysis of sandwich beam with functionally graded face sheets and porous core via point interpolation meshfree method based on polynomial basic function. Archive of Applied Mechanics. 2021;91(3):933–47.
17. Magnucki K, Magnucka-Blandzi E, Wittenbeck L. Three models of a sandwich beam: Bending, buckling and free vibration. Engineering Transactions. 2022;70(2):97-122.
18. Kustosz J, Magnucki K, Goliwąs D. Bending of a stepped sandwich beam: The shear effect. Engineering Transactions. 2022;70(4):373-390.

Krzysztof Magnucki: https://orcid.org/0000-0003-2251-4697
Joanna Kustosz: https://orcid.org/0000-0002-9408-2099
Damian Goliwąs: https://orcid.org/0000-0003-3280-0400